THE JOURNAL OF BIOLOGICAL CHEMISTRY VOL. 283, NO. 43, pp. 29215–29227, October 24, 2008

Epigenetic Regulation of HYAL-1 Hyaluronidase Expression

*IDENTIFICATION OF HYAL-1 PROMOTER**

Received for publication, February 11, 2008, and in revised form, June 30, 2008 Published, JBC Papers in Press, August 21, 2008, DOI 10.1074/jbc.M801101200

Vinata B. Lokeshwar[‡§¶1], Pablo Gomez[‡], Mario Kramer[‡2], Judith Knapp[‡2], Melissa A. McCornack[‖], Luis E. Lopez[‡], Nevis Fregien[§], Neetika Dhir[‡], Steve Scherer[**], David J. Klumpp[‡‡], Murugesan Manoharan[‡], Mark S. Soloway[‡], and Bal L. Lokeshwar[‡¶§§]

From the Departments of [‡]Urology, [§]Cell Biology and Anatomy, [¶]Sylvester Comprehensive Cancer Center, [§§]Radiation Oncology, University of Miami Miller School of Medicine, Miami, Florida 33101, [‖]Promega Corporation, Madison, Wisconsin 53711, the [**]Department of Molecular and Human Genetics Human Genome Sequencing Center, Baylor College of Medicine, Houston, Texas 77030, and the [‡‡]Department of Urology, Northwestern University, Feinberg School of Medicine, Chicago, Illinois 60611-3008

HYAL-1 (hyaluronoglucosaminidase-1) belongs to the hyaluronidase family of enzymes that degrade hyaluronic acid. HYAL-1 is a marker for cancer diagnosis and a molecular determinant of tumor growth, invasion, and angiogenesis. The regulation of HYAL-1 expression is unknown. Real time reverse transcription-PCR using 11 bladder and prostate cancer cells and 69 bladder tissues showed that HYAL-1 mRNA levels are elevated 10–30-fold in cells/tissues that express high hyaluronidase activity. Although multiple transcription start sites (TSS) for HYAL-1 mRNA were detected in various tissues, the major TSS in many tissues, including bladder and prostate, was at nucleotide 27274 in the cosmid clone LUCA13 (AC002455). By analyzing the 1532 base sequence 5′ to this TSS, using cloning and luciferase reporter assays, we identified a TACAAA sequence at position −31 and the minimal promoter region between nucleotides −93 and −38. Mutational analysis identified that nucleotides −73 to −50 (which include overlapping binding consensus sites for SP1, Egr-1, and AP-2), bases C^{-71} and C^{-59}, and an NFκB-binding site (at position −15) are necessary for promoter activity. The chromatin immunoprecipitation assay identified that Egr-1, AP-2, and NFκB bind to the promoter in HYAL-1-expressing cells, whereas SP1 binds to the promoter in non-HYAL-1-expressing cells. 5-Aza-2′-deoxycytidine treatment, bisulfite DNA sequencing, and methylation-specific PCR revealed that HYAL-1 expression is regulated by methylation at C^{-71} and C^{-59}; both Cs are part of the SP1/Egr-1-binding sites. Thus, HYAL-1 expression is epigenetically regulated by the binding of different transcription factors to the methylated and unmethylated HYAL-1 promoter.

The hyaluronidase (HAase)[3] family of endoglycosidases degrades hyaluronic acid (HA) into smaller fragments, some of which are angiogenic (1, 2). HA is a high molecular mass non-sulfated glycosaminoglycan that is made up of repeating disaccharide units, D-glucuronic acid and *N*-acetyl-D-glucosamine (3–5). In addition to its roles in absorbing water and maintaining osmotic balance, HA regulates cell adhesion, migration, and proliferation (5–7). There are six HAase genes found in the human genome. These genes occur in two clusters, and *HYAL-1*, *HYAL-2*, and *HYAL-3* genes are present in the chromosome 3p21.3 locus and *HYAL-4*, *HYAL-P1*, and *PH20* reside in the chromosome 7q31.3 locus (2, 8, 9).

Normally HYAL-1 is present in serum and urine; however, elevated concentrations are also found in tumor tissues and cells (10–18). In fact, HYAL-1 was the first tumor-derived HAase to be identified (19, 20). In bladder, prostate, and head and neck carcinomas, elevated HA and HYAL-1 levels are found in tumor cells, tissues, and related body fluids (*e.g.* urine for bladder cancer and saliva for head and neck cancer). Importantly, these levels have been shown to correlate with the aggressiveness of the tumor (12–18). For example, urinary HAase levels measured by the HAase test, have ~85% accuracy in detecting high grade bladder tumors, which have high invasive potential and worse prognosis (21–23). Urinary HA and HAase levels, measured by the HA-HAase test, have ~88% accuracy in detecting bladder cancer, regardless of the tumor grade and stage (21, 23). Furthermore, elevated HA and HAase expression in tumor tissues correlates with a positive HA-HAase test (13). HYAL-1 expression also serves as an accurate (86–88%) and independent prognostic indicator for disease progression in prostate cancer patients treated with radical prostatectomy (16, 17).

Recent work from our laboratory showed that HYAL-1 is a molecular determinant of tumor growth, invasion, and angiogenesis. Silencing HYAL-1 expression in bladder and prostate cancer cells results in cell cycle arrest and decreased invasive activity *in vitro*. In xenografts, silencing HYAL-1 expression causes a decrease in tumor growth, inhibition of infiltration into muscle, lymphatics, and the vasculature, and reduction in angiogenesis (24, 25). However, overexpression of HYAL-1 in tumor cells, at levels significantly higher than the

* This work was supported, in whole or in part, by National Institutes of Health Grants R01 072821-09 and R01 CA 123063-01 (NCI) (to V. B. L.). This work was also supported by Florida Department of Health Bankhead Coley Cancer Research Program Grant. The costs of publication of this article were defrayed in part by the payment of page charges. This article must therefore be hereby marked "*advertisement*" in accordance with 18 U.S.C. Section 1734 solely to indicate this fact.

[1] To whom correspondence should be addressed: Dept. of Urology (M-800), Miller School of Medicine, University of Miami, P. O. Box 016960, Miami, FL 33101. Fax: 305-243-6893; E-mail: vlokeshw@med.miami.edu.

[2] Supported by the International Academy of Life Sciences, Biomedical Exchange Program.

[3] The abbreviations used are: HAase, hyaluronidase; 5-AzaC, 5-Aza-2′-deoxycytidine; CHIP, chromatin immunoprecipitation; CM, conditioned medium; HA, hyaluronic acid; HA-oligo, hyaluronic acid oligosaccharides; TSA, trichostatin A; RT, reverse transcription; TSS, transcription start site; ELISA, enzyme-linked immunosorbent assay; RACE, rapid amplification of cDNA ends.

levels expressed in tumor cells or cancer tissues, induces apoptosis and inhibits tumor formation (25). Because both the overexpression and silencing of HYAL-1 expression inhibit tumor growth, it appears that HYAL-1 expression is tightly regulated in tumor tissues and cells, such that it promotes tumor growth and progression.

Only a few studies have examined the regulation of HAase expression. One study has identified the HYAL-2 promoter region and determined that its expression, at least in chondrocytes, is constitutive (26). One of the mechanisms of HYAL-1 regulation involves alternative mRNA splicing, which results in several splice variants that encode enzymatically inactive proteins (27). Recently, we have shown that one of the splice variants, HYAL1-v1, acts as a negative regulator of tumor growth, invasion, and angiogenesis (28). Selbi *et al.* (29) showed that bone morphogenetic protein-7 decreases HYAL-1 and HYAL-2 mRNA expression in renal proximal tubular cells, whereas Ohno *et al.* (30) showed that interleukin 1β increases HYAL-1 expression in periodontal ligament fibroblasts. Recently, Li *et al.* (31) showed that transforming growth factor-β1 increases HYAL-1 expression in dermal fibroblasts. With the exception of these few studies, which indicate some type of transcriptional regulation, little is known about the mechanisms by which the expression of HYAL-1 or any of the other HAase genes is regulated. In this study, we investigated whether HYAL-1 expression is regulated at the transcriptional or the translational level. In addition, we identified the minimal promoter region in the *HYAL-1* gene and examined its regulation by DNA methylation and transcription factor binding.

EXPERIMENTAL PROCEDURES

Materials—IQ™ Supermix, HYAL-1, and actin PCR primers and 5′-FAM/3′-BHQ-labeled HYAL-1 and actin probes were purchased from Bio-Rad, Sigma Genosys, and Integrated DNA Technology (Coralville, IA), respectively. Human Sure-RACE™ cDNA 5′ end discovery panel was purchased from Origene Technologies Inc. (Rockville, MD). pGL4.10[*luc2*] vector, pGL4.74[hRluc/TK] vector, and Dual-Glo™ luciferase assay system were purchased from Promega Corp. (Madison, WI). TOPO TA Cloning® kit (pCR®2.1-TOPO® vector), Superscript® II reverse transcription kit, and Platinum® *Taq*DNA polymerase (high fidelity) were purchased from Invitrogen. KpnI and NheI restriction endonucleases and M.SssI DNA methylase were purchased from PerkinElmer Life Sciences. Genomic DNA isolation kit, QIAquick® PCR purification kit, EpiTect®Bisulfite kit, and Effectene® transfection reagent were from Qiagen (Valencia, CA). MG132 was purchased from EMD Biosciences Inc. (San Diego, CA), and human genomic DNA was obtained from Clontech. Human umbilical cord HA was purchased from MP Biomedicals (Solon, OH). HA (1×10^6 Da) and HA oligosaccharides (HA-oligo) of average molecular mass 2,000 Da were purchased from Genzyme Corp. (Cambridge MA). Antibodies for the chromatin immunoprecipitation (CHIP) assay were bought from Santa Cruz Biotechnology Inc, Santa Cruz, CA (anti-NFκB, anti-Egr-1, anti-AP-2), and Millipore-Upstate, Billerica, MA (anti-SP1). 5-Aza-2′-deoxycytidine (5-AzaC) and trichostatin A (TSA) were purchased from Sigma.

Cell Culture and Tissues—Bladder (HT1376, UMUC-3, T24, J82, RT4, HT1197, and HT5637) and prostate (DU145 and LNCaP) cancer cells were purchased from American Type Culture Collection. 253J-Lung and 253J-Parent cells were kindly provided by Dr. Colin Dinney (M. D. Anderson Cancer Center, Houston, TX). PC3-ML cells were provided by Dr. Mark Stearns (Department of Pathology, Drexel University College of Medicine, Philadelphia, PA). All tumor cell lines were cultured in RPMI 1640 + 10% fetal bovine serum + gentamicin. Normal urothelial cells (TEU-1 and PD07i) were cultured in EpiLife/HKGS medium (Invitrogen) containing 200 μg/ml neomycin.

Inhibitor Treatments, Immunoprecipitation, Immunoblotting, and the HAase Activity Assay—Bladder cancer cells incubated in RPMI 1640 medium were treated with cycloheximide (10 μg/ml) for various time periods or with MG132 (2.5 μM) for 8 h. Following incubation, the culture conditioned media (CM) and the cell lysates were subjected to HYAL-1 immunoblotting using a rabbit anti-HYAL-1 IgG as described previously (19, 20, 28). The blots for the cell lysates were reprobed with an anti-actin antibody (BD Biosciences), as a loading control. Because there is no well accepted protein standard that can be used as a loading control for the CM, an equal amount of total protein (10 μg) was loaded for each sample. For sumoylation studies, HT1376 (1×10^6) cells were lysed in a RIPA buffer (50 mM Tris-HCl, pH 7.4, 150 mM NaCl, 0.5% Triton® X-100, 0.5% Nonidet P-40, 10 mM *N*-ethylmaleimide, and protease mixture). Then the cell lysates were immunoprecipitated using the anti-HYAL-1 IgG (28), and the immunoprecipitates were immunoblotted using an anti-sumo1 or an anti-sumo2/3 mouse monoclonal antibody (MBL, Nagoya, Japan). As a control, the HT1376 cell lysate, immunoprecipitated using normal rabbit IgG, was immunoblotted under similar conditions. HAase activity in the serum-free culture CM was measured using the HAase ELISA-like assay and normalized to milligrams/ml protein as described before (19, 20).

HYAL-1 Real Time RT-PCR—Total RNA was isolated from bladder cancer cells and tissues (~30 mg). In some cases, the cells were treated with actinomycin-D (2 μM), and total RNA was prepared at different time intervals. Alternatively, to test the effect of HA or HA-oligo (~2 kDa) on HYAL-1 mRNA expression, HT1376 cells cultured in 6-well plates were serum-starved for 24 h. The cells were then treated with various concentrations (0–50 μg/ml) of HA or HA-oligo for 0, 4, 8, 14, and 24 h. Total RNA was prepared from treated and untreated cells. Total RNA from various samples was reverse-transcribed, and the cDNAs were subjected to real time PCR as described before (32), using HYAL-1(1746L) and HYAL-1(1886R) primers and a 5′-FAM/3′-BHQ labeled HYAL-1(1841) probe (Table 1). HYAL-1 mRNA levels were normalized to β-actin and expressed as $1/2^{\rho Ct} \times 10{,}000$, as described before (32).

Mapping of HYAL-1 Transcription Start Site—The human Sure-RACE Discovery panel contains 24 RACE-ready tissue-specific cDNAs, each of which were subjected to nested PCR using two sets of PCR primers as follows: set 1, ADP1/HYAL-1(1919R), and set 2, ADP2/HYAL-1(666R). The sequences of all primers used in this study are shown in Table 1. PCR products were cloned into the pCR2.1-TOPO vector and sequenced. To determine the TSS in bladder tissues and cells, cDNAs were

TABLE 1

Sequences of the primers used for RT-PCR and generating promoter constructs

The numbering for forward L-primers and reverse R-primers is based on the TSS at position 1 (base 27274 in the cosmid clone LUCA13 from 3p21.3 accession number AC002455). The sequences for the primers ADP1 and ADP2 primers were provided in the Human Sure-RACE panel kit. As indicated, a KpnI (GGTACC) or NheI (GCTAGC) restriction site was added on some of the primers, and it is underlined in the primer sequence.

Name	Forward L-primers	Name	Reverse R-primers
ADP1	5′-CGGAATTCGTCACTCAGCG-3′	HYAL-1(1919R)	5′-ATCACCACATGCTCTTCCGC-3′
ADP2	5′-AGCGCGTGAATCAGATCG-3′	HYAL-1(666R)	5′-TCGAGTAAGGTCAGGAAGAG-3′
+1L	5′-CTTCCTCCAGGAGTCTCTGGT-3′	+410R	5′-GCTAGCCACATCCGAGTTGCCTCTCA-3′
−30L	5′-ACAAAAGCTCAGAATTTCCA3′	+84R (with NheI linker)	5′-GCTAGCTCCAAATTTCCTGACCCCAG-3′
−23L	5′-CTCAGAATTTCCAGCAGCGG-3′	+84R (with KpnI linker)	5′-GGTACCTCCAAATTTCCTGACCCCAG-3′
−1532L	5′-GGTACCGAGGCAATGGAGGCAATCAT-3′	+612R	5′-GCTAGCCGGGACTGGTCGAGGACAAC-3′
−1326L	5′-GGTACCGGATCTCATGCTCACAAGAC-3′		**Real Time PCR primers and probe**
−1150L	5′-GGTACCTGACTTCATGAACACAGTGC-3′	HYAL-1 (1746L)	5′-AAGCCCTCCTCCTCCTTAACC-3′
−853L	5′-GGTACCGTCTTGCTACATTGCCTAGG-3′	HYAL-1 (1886R)	5′-AGCCAGGGTAGCATCGAC-3′
−663L	5′-GGTACCGTAGCACAGTGGAGCAGTCT-3′	HYAL-1 (1841 Probe)	FAM5′-CAGGCACAGATGGCTGTGGAGTT3′-BHQ
−452L	5′-GGTACCAAGTGCTAGGATTATAGGCG-3′	−224(BS)L	5′-TTTTAGTTTAGGTAAGGTTATAAAGTTTTG-3′
−146L	5′-GGTACCAACCAAGATCCCTTTGCCAG-3′	+25(BS)R	5′-CTACACCAAAAACTCCTAAAAAAAA-3′
−93L (with KpnI linker)	5′-GGTACCCCTGGCCTCCTAATCCAAGG-3′	M(−70) Probe	FAM5′-TCGTTTTTTGGTTCGTTTTTGGTTTGGGTGG3′-BHQ
−93 L (with NheI linker)	5′-GCTAGCCCTGGCCTCCTAATCCAAGG-3′	UM(−70) Probe	FAM5′-TTGTTTTTTGGTTTGTTTTTGGTTTGGGTGG-3′-BHQ
−38L	5′-GGTACCGACCCCCTACAAAAGCTCAG-3′		

subjected to PCR using the HYAL-1(666R) primer and one of the forward primers, +1L, −23L, or −30L, to detect HYAL-1 transcripts starting at −30, −23, +1, or +5. PCR products (if generated) were cloned into the pCR2.1-TOPO vector and sequenced.

Generation of HYAL-1 Promoter-Reporter Constructs—HYAL-1 genomic sequence, up to 1532 nucleotides upstream of the HYAL-1 TSS, was PCR-amplified using the −1532L/HYAL-1(666R) primer pair and human genomic DNA as a template (Table 1). The PCR product was cloned into the pCR2.1-TOPO vector. Using this HYAL-1 sequence as the template, 13 HYAL-1 genomic constructs were generated by PCR using the primer pairs listed in Table 1. The forward primers contained a KpnI restriction site at the 5′ end, and the reverse primers contained an NheI site. Each PCR product was cloned into the pGL4.10[*luc2*] vector between the KpnI and NheI restriction sites, using a two-step cloning process, in which the first step involved the cloning of each PCR product into the pCR2.1-TOPO vector. The position of each construct is described relative to the TSS (+1) in the bladder tissues and cells.

Generation of HYAL-1 Oligonucleotide Mutants—The HYAL-1 sense and antisense oligonucleotides containing the −80 to +17 sequence were custom-synthesized with a KpnI or a NheI restriction site, respectively. Each oligonucleotide contained either a desired mutation or no mutation (wild type). Following annealing, the double-stranded oligonucleotides were cloned into the pGL4.10[*luc2*] vector.

Transient Transfection and Luciferase Reporter Assay—Bladder and prostate cells cultured in 96-well plates were transiently transfected with a HYAL-1 promoter-firefly luciferase reporter construct or an oligonucleotide-firefly luciferase reporter construct, together with a *Renilla* luciferase normalization vector, using the Effectene transfection reagent. Following 48 h of incubation, firefly and *Renilla* luciferase activities were measured using the Dual-Glo assay, as per the manufacturer's instructions. To test the effect of HA or HA-oligo on the promoter activity of HYAL-1 promoter mutants, HT1376 and T24 cells were transiently transfected with wild type or a HYAL-1 promoter mutant construct. 24 h following transfection, the cells were incubated in serum-free RPMI 1640 medium for 24 h and then with HA/HA-oligo (20 μg/ml) for 14 h. HYAL-1 promoter activity was determined as described above. The promoter activity of the HYAL-1 wild type promoter construct was designated as 100%, and the promoter activity of the wild type construct in HA-treated cells and of the mutant constructs in HA-treated and untreated cells was expressed as a percentage of the wild type untreated construct. The statistical significance of the observed change in the HYAL-1 promoter activity, by the various treatments, was examined by the Bonferroni's multiple comparison test.

Chromatin Immunoprecipitation (CHIP) Assay—CHIP assays were performed using the EZ-CHIP™ kit (Millipore Corp., Billerica, MA) and a protocol supplied by the manufacturer with some modifications (32). Briefly, $\sim 2 \times 10^7$ cells were fixed in 0.5% formaldehyde for 10 min to cross-link bound proteins, lysed in SDS lysis buffer, and sonicated to yield chromatin fragments between 200 and 1000 bp. The cell lysates ($\sim 1 \times 10^6$ cells) were immunoprecipitated using anti-SP1, anti-Egr-1, anti-AP-2, or anti-NFκB antibody or normal rabbit IgG (control antibody). Immunoprecipitation using anti-RNA polymerase IgG was included as a positive control (supplied in the kit). Following immunoprecipitation, the bound chromatin (beads) and unbound chromatin (supernatant) were separated. Following washing of the beads to remove nonspecifically bound proteins, the cross-linking was reversed in the bound, unbound, and input (sonicated cell lysate) samples, and the immunoprecipitated protein was digested with proteinase K. DNA was purified and subjected to real time PCR using −146L and +84R primers. PCR was performed for 50 cycles at an annealing temperature of 64 °C for both HYAL-1 and the positive control (glyceraldehyde-3-phosphate dehydrogenase primers). A standard curve was prepared using serial dilutions of the −146/+84 promoter construct. The amount of HYAL-1 promoter that was present in the bound and unbound (or input) fractions was calculated from the standard curve. The amount of HYAL-1 promoter in the unbound and the input fractions was very similar. The results were expressed as (bound ÷ input) $\times 10^4$. Alternatively, the results were expressed as (1/fold difference) $\times 10^4$, where the fold difference is $2^{(Ct \text{ bound} - (Ct \text{ input or unbound})}$. The results obtained by both methods were similar. The latter method is advantageous and perhaps more accurate, because the results are calculated from the actual *Ct* values and not from the amount of HYAL-1 PCR product pres-

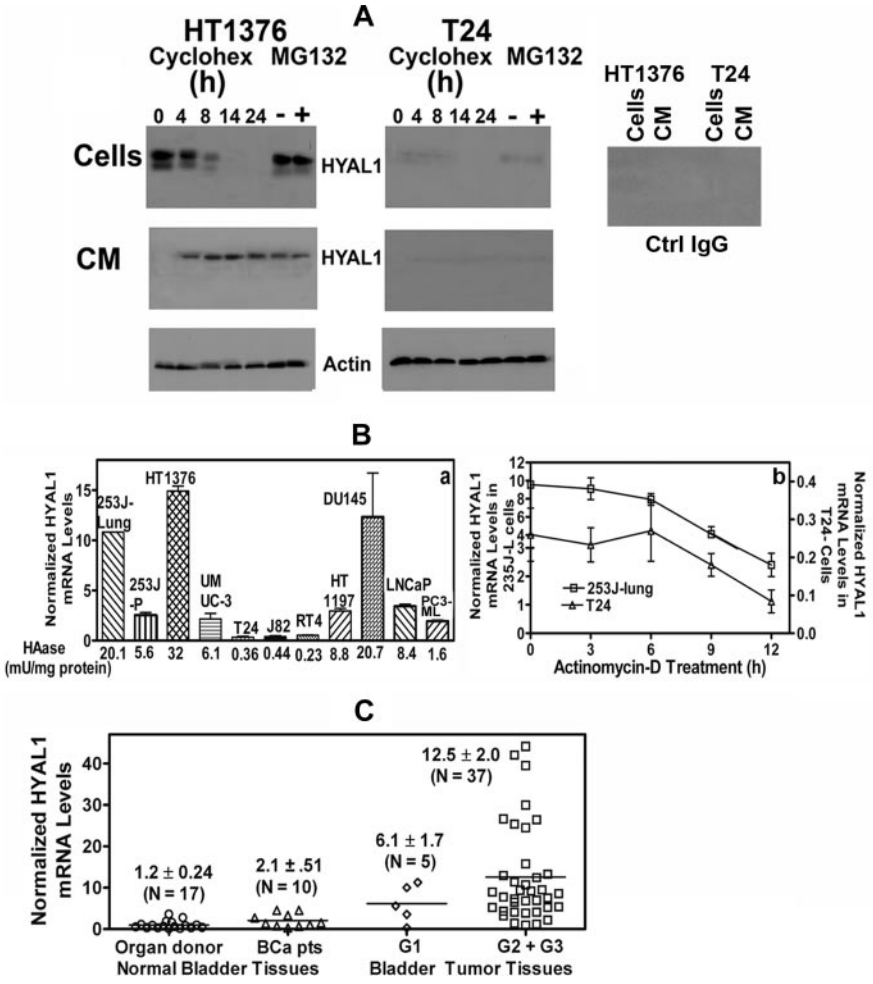

FIGURE 1. **Determination of the translational and transcriptional regulation of HYAL-1 expression.** *A,* analysis of HYAL-1 protein levels. HT1376 and T24 cells were treated with cycloheximide (*Cyclohex*) or MG132 and HYAL-1 protein levels in cell lysates, and conditioned media (*CM*) were examined by immunoblotting. Loading control for cell lysates, actin. For CM, equal amount of total protein (10 μg) was analyzed. Control IgG immunoblot was performed using cell lysates from time 0 and CM from 14-h time point, using normal rabbit IgG. *B,* measurement of HYAL-1 mRNA levels. *Panel a,* HYAL-1 mRNA levels were measured in various bladder and prostate cancer cell lines by real time RT-PCR, as described under "Experimental Procedures." HYAL-1 mRNA levels normalized to β-actin mRNA levels are shown. HAase activity secreted in CM was measured by HAase ELISA-like assay and was normalized to total protein. *Panel b,* 253J-Lung and T24 cells were treated with actinomycin D, and HYAL-1 mRNA levels were measured by real time RT-PCR at indicated time intervals. *C,* HYAL-1 mRNA levels were measured by real time RT-PCR on total RNA isolated from bladder tissues. HYAL-1 mRNA levels normalized to β-actin mRNA levels for individual tissues, as well as mean ± S.E. HYAL-1 mRNA levels per category are shown.

ent in each sample, as determined by the extrapolations from the standard graph. To examine the effect of HA on transcription factor binding, HT1376 cells were incubated in serum-free RPMI 1640 medium for 24 h and then treated with HA (20 μg/ml) for 14 h. CHIP assay was conducted on both HA-treated and untreated cells. The results were expressed as a percentage of the untreated, *i.e.* for each IgG (1/fold difference) $\times 10^4$ of the untreated sample was considered as 100% and the (1/fold difference) $\times 10^4$ of the HA-treated sample was expressed as a percentage of the untreated.

5-AzaC and TA Treatment—T24 and J82 cells cultured in 12-well plates were treated with 5-AzaC (0–2.5 μM) continuously for 96 h, and in some samples 100 nM TSA was added for the last 16 h. RNA was isolated and subjected to HYAL-1 real time RT-PCR. For HAase activity determination and HYAL-1 immunoblotting, the growth medium was removed after 60 h and replaced with serum-free RPMI 1640 medium. HAase activity was determined by the HAase ELISA-like assay.

Bisulfite Treatment and Methylation-specific Real Time PCR—Genomic DNA was isolated from bladder and prostate cells and subjected to bisulfite treatment using the EpiTect® bisulfite kit. This treatment converts unmethylated cytosine to uracil, whereas the 5-methylcytosine remains unchanged (34). Following bisulfite treatment, DNA was purified, and the HYAL-1 promoter region was amplified using the −224(BS)L and +25(BS)R primers. The amplified HYAL-1 promoter fragment was purified using the QIAquick® PCR purification kit and then sequenced using the −224(BS)L primer. Alternatively, bisulfite-treated DNA was subjected to real time PCR using −224(BS)L and +25(BS)R primers and the M(−70) or UM(−70) probe. The M(−70) and UM(−70) probes were used to selectively detect HYAL-1 promoter methylated or unmethylated at C^{-71} and C^{-59}. The −93/+84 construct was methylated *in vitro*, using M.SssI DNA methylase (PerkinElmer Life Sciences) and then subjected to bisulfite treatment for use as a positive control for the methylated DNA. The bisulfate-treated −93/+84 construct was used as a positive control for the unmethylated DNA. The results were expressed as (UM ÷ (M + UM)) × 100.

RESULTS

Transcriptional Regulation of HYAL-1 Expression—HYAL-1 expression is elevated in invasive cancer cell lines and in tumor tissues (12–22). However, little is known whether HYAL-1 expression is controlled at the transcriptional or translational levels, or both. Therefore, we investigated whether the up-regulation is because of differences in protein synthesis and/or degradation among low and high HYAL-1-expressing cells. We analyzed HYAL-1 expression in cell lysates and CM, after the treatment of HT1376 (high HYAL-1 expresser) and T24 (low HYAL-1 expresser) bladder cancer cells with either cycloheximide, a protein synthesis inhibitor, or MG132, a reversible ubiquitin 26 S proteosome inhibitor. As shown in Fig. 1*A*, the HYAL-1 protein level in T24 cells is >10-fold lower than the level in HT1376 cells. In the cell lysates two protein bands are detected by the anti-HYAL-1 IgG. These proteins are HYAL-1 related, because the control IgG does not detect either

band (Fig. 1*A*). In the cell lysates, HYAL-1 protein disappears at about 8 h. This could either be due to its degradation or secretion into the CM. Immunoblot analysis of the CM shows that HYAL-1 is present in the CM and that the protein is stable beyond 24 h. Although the differences exist between the amount of HYAL-1 protein expressed in HT1376 and T24 cells, HYAL-1 protein processing appears to be similar in both cell types (Fig. 1*A*). The difference in the two cell lines with respect to HYAL-1 protein levels is not because of the ubiquitin-mediated degradation of HYAL-1 protein, as the MG132 treatment did not increase HYAL-1 levels in the cell lysates or culture CM from either cell types (Fig. 1*A*). No sumoylation sequence is found in the HYAL-1 protein (33). Consistent with this observation, HYAL-1 immunoprecipitation, followed by anti-sumo1 or anti-sumo2/3 immunoblotting, showed that HYAL-1 protein is not sumoylated (data not shown). These results show that the differences in HYAL-1 expression among different cell lines are very likely not at the protein synthesis or degradation level.

To determine whether high and low HYAL-1-expressing cells show differences at HYAL-1 mRNA levels, we performed real time RT-PCR analysis. As shown in Fig. 1*B, panel a*, HYAL-1 mRNA levels are 10–30-fold elevated in bladder and prostate cancer cells, which express high HAase activity and HYAL-1 protein (19, 20). To determine whether the differences in HYAL-1 mRNA levels in high and low HYAL-1-expressing cells are because of the differences in HYAL-1 mRNA degradation, the rate of HYAL-1 mRNA degradation was determined by treating 253J-Lung and T24 cells with actinomycin-D, an mRNA synthesis inhibitor. Fig. 1*B, panel b*, shows that although 253J-Lung cells express 30-fold higher HYAL-1 mRNA levels than T24 cells, the rate of HYAL-1 mRNA degradation (normalized to β-actin) among both cell lines is similar; $t_{1/2} \sim 10$ h. It is noteworthy that because the HYAL-1 mRNA levels were normalized to β-actin levels at each time point, the levels did not reach "zero" even at 12 h. This is because the β-actin mRNA levels also decreased in a time-dependent manner. The time course could not be conducted beyond 12 h, because the actinomycin D treatment became cytotoxic at later time periods. HYAL-1 mRNA levels are also elevated by 5–12-fold in bladder tumor tissues when compared with normal bladder tissues obtained either from organ donors or histologically normal bladder tissues obtained from patients with bladder tumors (Fig. 1*C*). The differences in the HYAL-1 mRNA levels between normal and bladder tumor tissues are statistically significant ($p < 0.001$; Dunn's multiple comparison test; nonparametric distribution). These results show that the control of HYAL-1 expression is at least partly at the transcriptional level.

Identification of TSS for HYAL-1—To better understand the control of HYAL-1 expression, we embarked on identifying the promoter element(s) in the HYAL-1 gene. To map the promoter element(s) in the HYAL-1 gene, we first determined the TSS for HYAL-1 mRNA using the human Sure-RACE discovery panel. As shown in Fig. 2*A*, HYAL-1 mRNA is detected in several tissues, excluding normal prostate, breast (very low expression), pituitary, and peripheral blood leukocytes. The cloning and the sequencing of the RACE-PCR products generated in each of the remaining tissues showed several TSS (Table 2 and Fig. 2*B*). The TSS at nucleotide 1 (Fig. 2*B*) corresponds to base 27274 in the human cosmid clone LUCA13 (accession number AC002455). Except for the transcripts which begin at TSS +377 or +550, the region between +109 and +596 is spliced out in all HYAL-1 transcripts that were detected in various tissues. In the transcript beginning at −450, which was found in fetal brain, the nucleotides between −210 and +596

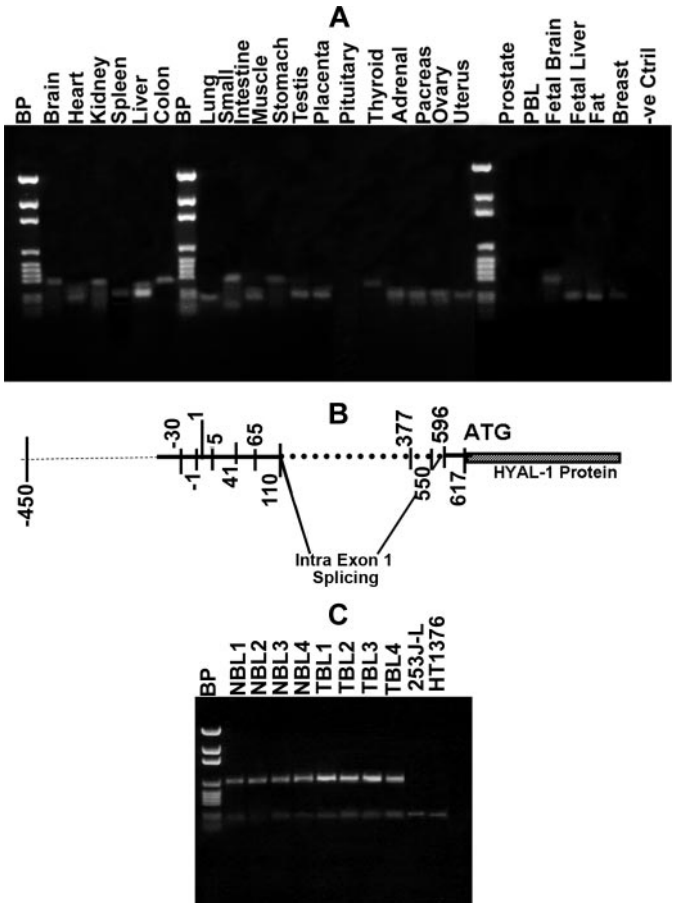

FIGURE 2. **Determination of transcription start site(s) for HYAL-1.** *A,* human Sure-RACE panel involving 24 tissues was used to determine the TSS for HYAL-1 mRNA, using RT-PCR. PCR products were analyzed by agarose gel electrophoresis and ethidium bromide staining. Molecular markers, pGEM (Promega). *B,* schematic representation of HYAL-1 gene showing various TSS (−450, −30, −2, +1, +5, +41, +65, +377, and + 550) identified using the human Sure-RACE panel, alternatively spliced region (—) and the translational start site. *C,* RT-PCR analysis of normal bladder (*NBL*) and bladder tumor (*TBL*) tissues and bladder cancer cells using the +1L and HYAL-1(666R) primer pair.

TABLE 2

Tissue distribution of HYAL-1 transcripts with different TSS

HYAL-1 transcripts expressed in each of the 24 tissues in the Sure-RACE panel were cloned and sequenced to determine the TSS for each transcript. The position of each TSS is indicated with respect to the base 27274 (TSS +1) in the human cosmid clone LUCA13 (accession number AC002455).

TSS	Tissue
−450	Fetal brain
−30	Kidney, brain
−1	Adrenal, liver, small intestine, spleen
+1	Muscle, pancreas, uterus, ovary, lung, placenta, testis
+5	Liver, lung, heart, breast
+41	Fetal liver
+65	Liver
+377	Colon, small intestine, thyroid, colon
+550	Fetal liver, fat

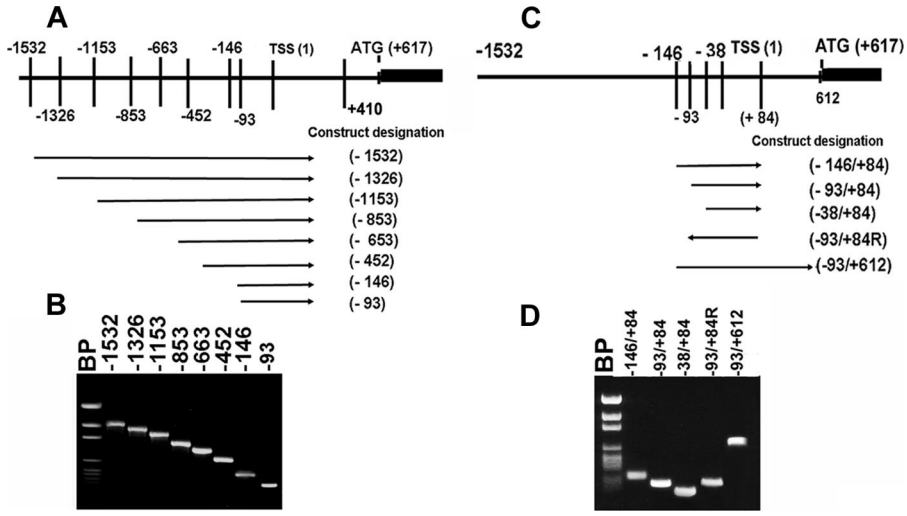

FIGURE 3. **Generation of HYAL-1 promoter constructs.** *A,* schematic representation of various HYAL-1 promoter constructs starting at different 5′ positions and ending at +410 position. The numbers in the *parentheses* indicate the starting position of each construct 5′ to the TSS designated as "1." *B,* PCR amplification of various constructs shown under "*A*" using different forward primers with KpnI linker and the +410R primer with NheI linker. The sequences of these primers are shown in Table 1. *C,* schematic representation of various HYAL-1 promoter constructs. The *arrows* and the *numbers* in parentheses indicate the starting and the ending position of each construct. −93/84R is the reverse construct in which HYAL-1 promoter was cloned in reverse orientation with respect to luciferase cDNA. *D,* PCR amplification of various constructs shown under *C* using various forward and reverse primer pairs as shown in Table 1.

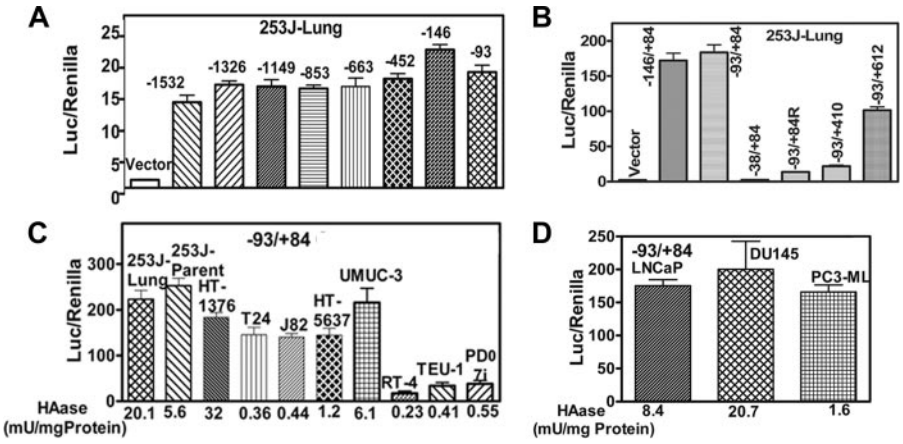

FIGURE 4. **Analysis of HYAL-1 promoter-reporter constructs.** *A,* 253J-Lung cells were transiently co-transfected with a *Renilla* vector and an HYAL-1 promoter-luciferase construct starting at a specific 5′ position and ending at +410 at the 3′ end, as described under "Experimental Procedures." Firefly luciferase activity (luc2) was measured and normalized to *Renilla* luciferase (hRluc). Normalized reporter activity (ratio of firefly luciferase to *Renilla* luciferase (*Luc/Renilla*)) is shown. *B,* normalized reporter activity induced by various HYAL-1 promoter constructs was assayed in 253J-Lung cells following transient transfection. *C,* reporter activity induced by the −93/+84 construct was assayed in various bladder cell lines following a transient co-transfection, as described above. In the same assay, the vector construct was also co-transfected in each cell line along with the *Renilla* luciferase vector. The normalized basal reporter activity from the vector construct varied between 0.8 and 3.1 in various cell lines. *D,* reporter activity induced by the −93/+84 construct was assayed in prostate cancer cell lines following a transient co-transfection. The normalized basal reporter activity from the vector construct varied between 1.2 and 2.5 in the three cell lines.

were spliced out. These results show that, although there are multiple TSS in the HYAL-1 gene, the transcription predominantly starts between nucleotides −1 and +5.

Because bladder tissue was not included in the Sure-RACE discovery panel, we subjected bladder tissues (normal and tumor) and bladder cancer cells to RT-PCR using PCR primers that amplify cDNAs starting at +1 or +5 (primer pair +1L and HYAL-1(666R), see Table 1). As shown in Fig. 2*C*, two PCR products of 666 and 181 bases are generated in bladder tissues and bladder cancer cells using this primer pair. Sequencing of both PCR products revealed that the TSS is at (or upstream of) nucleotide +1. As described before (27), the 666-base PCR product is the unspliced HYAL-1 transcript. The 181-base product is generated by splicing the region between nucleotides 109 and 596 present within the 5′-untranslated region of the HYAL-1 transcript (27, 35). RT-PCR was also performed using primers that can amplify a cDNA starting at −30 (primer pair −23L or −30L and HYAL-1(666R), see Table 1). However, no PCR product was observed using these primers (data not shown).

Examination of the Minimal Promoter Region in HYAL-1—To determine the minimal HYAL-1 promoter region, we cloned up to ~1.5-kb region upstream of the HYAL-1 TSS (position +1), using a firefly luciferase reporter vector and a two-step cloning strategy. We initially generated eight HYAL-1 genomic fragments by PCR amplification. The positions of these genomic fragments and the PCR products are shown in Fig. 3, *A* and *B*. These fragments were cloned into the pGL4.10[*luc2*] vector, and the firefly luciferase activity was measured following the transfection of 253J-Lung cells with each construct. As shown in Fig. 4*A*, all of the constructs, including the smallest construct (−93/+410), induce promoter activity 15–20-fold over the basal reporter activity induced by the promoterless pGL4.10[*luc2*] vector (vector construct). To identify the minimal promoter region, we generated three new constructs, −146/+84, −93/+84, and −38/+84 (Fig. 3, *C* and *D*). As shown in Fig. 4*B*, the −146/+84 and −93/+84 constructs induce 170–180-fold more reporter activity than the vector construct, but the −38/+84 construct has the same reporter activity as the vector construct. Therefore, the minimal promoter activity in the HYAL-1 gene is between nucleotides −93 and −38. Cloning of the −93/+84 construct, in the reverse orientation with respect to the firefly luciferase gene, sharply decreases the reporter activity from ~180-fold to just ~10-fold higher than the basal reporter activity induced by the pGL4.10[*luc2*] vector (Fig. 4*B*). This suggests that the region −93 to −38 contains and is essential for the HYAL-1 promoter activity.

Because the −93/+84 construct induces ~170-fold more reporter activity than the vector, but the −93/+410 construct induces the reporter activity only ~20-fold over the control, this suggests two possibilities. First, a negative regulatory element(s) may be present within the +84 to +410 region, resulting in the loss of luciferase activity. Second, improper splicing of the HYAL-1-luciferase transcript may occur, causing the loss of the luciferase coding region. Although the +410 constructs contain the +109 splice donor site, they lack the +592 (AGGT) splice acceptor site present within the 5′-untranslated region of the HYAL-1 transcript. To test these two possibilities, we generated the −93/+612 construct (Fig. 3, *C* and *D*) that contains both the splice donor and acceptor sites of the HYAL-1 transcript. As shown in Fig. 4*B*, the −93/+612 construct induces ~80-fold more reporter activity than the vector construct. In the pGL4.10[*luc2*] sequence, 10 AGGT sites are found, and the nucleotides (AGCC) preceding the AGGT site at nucleotide 1613 in the pGL4.10[*luc2*] sequence are similar to those preceding the acceptor site at +592 (GGCC) in the HYAL-1 sequence. RT-PCR of the total RNA isolated from 253J-Lung cells transfected with −146/+410 construct, using +1L and pGL4.10[*luc2*]1758R primers, resulted in a smear of PCR products with a major PCR band of ~300 bases (data not shown). This suggests that the modest reporter activity induced by various +410 constructs is most likely because of improper splicing and not because of the negative regulation of HYAL-1 promoter activity by sequences present within the +84 and +410 region.

Examination of HYAL-1 Promoter-Reporter Activity in Bladder and Prostate Cell Lines—Because the minimal promoter region was found to reside between nucleotides −93 and −38, we next examined whether the −93/+84 construct is able to induce the firefly luciferase reporter activity in bladder and prostate cancer cell lines. As shown in Fig. 4*C*, in the RT4 bladder cancer cell line and the TEU-1 and PD07i normal urothelial cell lines, the reporter expression following transfection with the −93/+84 construct is ~20-fold higher than the basal expression. However, in all other bladder cancer cell lines, the reporter activity of the −93/+84 construct is 150–230-fold over the basal activity, regardless of the endogenous HYAL-1 expression and HAase activity production (Fig. 4*C*). Similarly in prostate cancer cells, PC3-ML which express low HYAL-1 mRNA levels and HAase activity, the −93/+84 construct induced reporter activity (~170-fold) that is comparable with LNCaP and DU145 cells, which express HYAL-1 (Fig. 4*D*).

Identification of Putative HYAL-1 Promoter Transcription Factor Binding Sites—Because we experimentally identified the region between −93 and −38 as the minimal promoter region, we examined whether promoter analysis programs identify a similar region as the promoter in HYAL-1 gene. We used two promoter analysis programs, "www tools for promoter scan" (www-bimas.cit.nih.gov) and "Genomatix MatInspector." Both programs identified a putative promoter region in the HYAL-1 gene between nucleotides −262 and −12, which includes the experimentally identified HYAL-1 promoter region. The programs identified a TATA-box like sequence (TACAAA) at −31, overlapping binding sites for transcription factors Egr-1, SP1, and AP-2 between

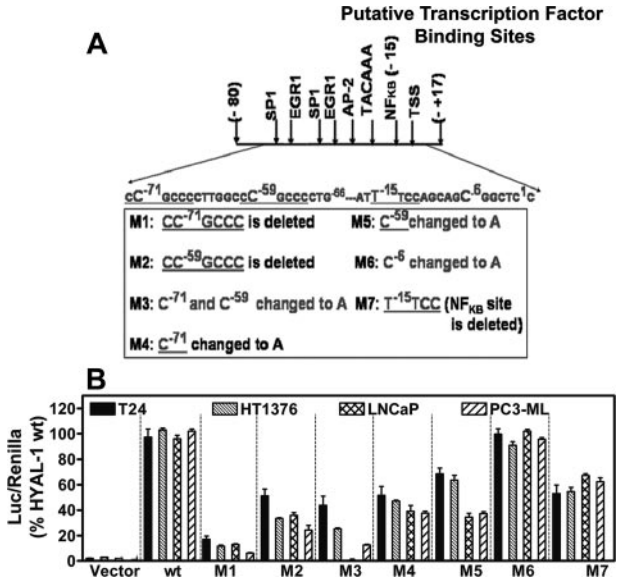

FIGURE 5. **Determination of luciferase activity induced by HYAL-1 promoter mutants.** *A,* schematic representation of the minimal HYAL-1 promoter region illustrating the putative transcription factor binding sites and of the oligonucleotide mutagenesis for generating seven HYAL-1 promoter mutants. The position of each mutant is shown. *B,* T24, HT1376, LNCaP, and PC3-ML cells were transiently transfected with vector, wild type (*wt*) (oligonucleotide −80 to +17 construct), or an oligonucleotide mutant, together with the *Renilla* vector. Firefly luciferase and *Renilla* luciferase activities were measured. In each cell line, the normalized firefly luciferase activity (promoter activity) for the wild type construct is considered as 100%,and promoter activity of each mutant is expressed as percent of HYAL-1 wild type.

nucleotides −73 and −50 and an NFκB-binding site at −15 (Fig. 5*A*). No CpG island was found within the predicted promoter region, but three CpGs were found at −71, −59, and −6.

To determine whether the region containing the transcription factor binding sites (*i.e.* −73 to −50 and −15) and the CpG dinucleotides (−71, −59, and −6) are important to promoter activity, we performed oligonucleotide-based mutagenesis. We synthesized a wild type oligonucleotide containing the region between −80 and +17 and also seven mutated oligonucleotides encompassing the same region (Fig. 5*A*). These oligonucleotides were cloned into the same firefly luciferase reporter vector, pGL4.10[*luc2*]. As shown in Fig. 5*B*, the wild type oligonucleotide resulted in reporter activity (~100–120-fold) that is comparable with the −93/+84 construct in bladder cancer (T24 and HT1376) and prostate cancer (LNCaP and PC3-ML) cell lines. This suggests that the region between −80 and +17 nucleotides is sufficient for HYAL-1 promoter activity. In mutants M1 and M2, one of the two CCGCCC sites (consensus for Egr-1/SP1-binding sites) was deleted. As shown in Fig. 5*B*, deletion of the $CC^{-71}GCCC$ site (M1) results in >90% loss of promoter activity in all four cells lines. Although not as drastic as M1 mutation, the deletion of the $CC^{-59}GCCC$ (M2) site also results in the loss of promoter activity (50–70%). It is noteworthy that in prostate cancer cell lines, mutation of both C^{-71} and C^{-59} results in a greater loss of promoter activity (>90% loss) than in bladder cancer cell lines (65–70% loss; Fig. 5, *A* and *B*). In both bladder and prostate cancer cell lines, mutant M4 (mutation of C^{-71} to A^{-71}) has 50–60% lower reporter activity

when compared with the wild type construct (Fig. 5, *A* and *B*). Some difference is observed in prostate and bladder cancer cell lines with respect to the mutation of C^{-59} (mutant 5). Whereas in prostate cancer cell lines M5 shows 60–70% loss of the promoter activity, in bladder cancer cell lines the loss is 30–40%. Contrary to the effect of C^{-71} and C^{-59} mutations on the reporter activity, alteration of C^{-6} to an A, does not cause any loss of reporter activity. Finally, the deletion of the putative NFκB site also results in 40–50% loss of the promoter activity. Therefore, although some differences exist among cell lines, the region between nucleotides −73 and −50 nucleotides and the putative NFκB-binding site appear to be important for HYAL-1 promoter activity in both prostate and bladder cancer cell lines.

Identification of Transcription Factors That Bind to HYAL-1 Promoter—To determine whether any of the transcription factors (*e.g.* SP1, AP-2, Egr-1, and NFκB) that have putative binding sites within the minimal HYAL-1 promoter region actually bind the promoter, we performed the CHIP assay. As shown in Fig. 6*A*, in 253J-Lung and HT1376 bladder cancer cell lines, which show high HYAL-1 expression, transcription factors Egr-1, AP-2, and NFκB bind the HYAL-1 promoter. However, there is no SP1 binding to the promoter (Fig. 6*A*). As expected, little HYAL-1 promoter binding is detected in the control IgG sample. The difference in Egr-1, AP-2, or NFκB binding to the HYAL-1 promoter, when compared with control IgG, was statistically significant ($p < 0.001$; Bonferroni's test). The binding of Egr-1 to the HYAL-1 promoter is 5-fold higher than of AP-2 or NFκB binding, and this difference is also statistically significant ($p < 0.01$). In LNCaP cells, which have some HYAL-1 mRNA expression (Fig. 1), only AP-2 binding is observed to the HYAL-1 promoter. The CHIP assay on HYAL-1 nonexpressing cells showed a different pattern of transcription factor binding. In T24, J82, HT5637, and PC3-ML cells, which do not express HYAL-1, SP1 binds to the HYAL-1 promoter (Fig. 6*B*). The difference in SP1 binding to the HYAL-1 promoter, when compared with control IgG, was statistically significant ($p < 0.001$; Bonferroni's test). No Egr-1, AP-2, or NFκB binding was observed to the HYAL-1 promoter in the T24, J82, or HT5637 cells. In PC3-ML cells, AP-2 bound the HYAL-1 promoter; however, SP1 binding was 4-fold higher than AP-2 binding ($p < 0.001$). Real time PCR results were confirmed by analyzing the PCR-amplified product on agarose gel, along with a HYAL-1 promoter standard amplified in the same experiment. As shown in Fig. 6*C*, an expected 230-bp HYAL-1 promoter PCR product (−146/+84) is detected in the anti-Egr-1, anti-NFκB, and/or anti-AP-2 real time PCR samples from 253J-Lung cells. In T24 cells, the PCR-amplified HYAL-1 promoter product is detected only in the anti-SP1 real time PCR sample.

Regulation of HYAL-1 Expression by DNA Methylation—Because similar reporter activity of HYAL-1 promoter constructs was detected in bladder and prostate cells, regardless of the endogenous HYAL-1 expression, and different transcription factors were found to bind to the promoter in HYAL-1-expressing and in HYAL-1 nonexpressing cells, we examined whether promoter methylation (at C^{-71}, C^{-59}, and possibly C^{-6}) regulates HYAL-1 expression. Therefore, we treated T24 and J82 cells for 4 days with a DNA-demethylating agent, 5-AzaC. HYAL-1 mRNA expression was determined by real time RT-PCR. The cell CM were assayed for HAase activity using the HAase test, and HYAL-1 protein expression was analyzed by immunoblotting. As shown in Fig. 7*A*, 5-AzaC treatment induces HYAL-1 mRNA expression in T24 and J82 cells, in a dose-dependent manner, with a maximum ~4-fold increase observed at ≥1 μM concentration. Methylated DNA binds methylcytosine-binding proteins, which in turn interact with histone deacetylases to silence gene expression (36). Consistent with this finding, when TSA, a histone deacetylase inhibitor, was combined with 5-AzaC, ~10-fold induction of HYAL-1 mRNA expression was observed in both the T24 and J82 cells (Fig. 7*A*). However, TSA alone did not induce HYAL-1 expression (data not shown). The increase in HYAL-1 mRNA expression is accompanied by an increase in HAase activity and

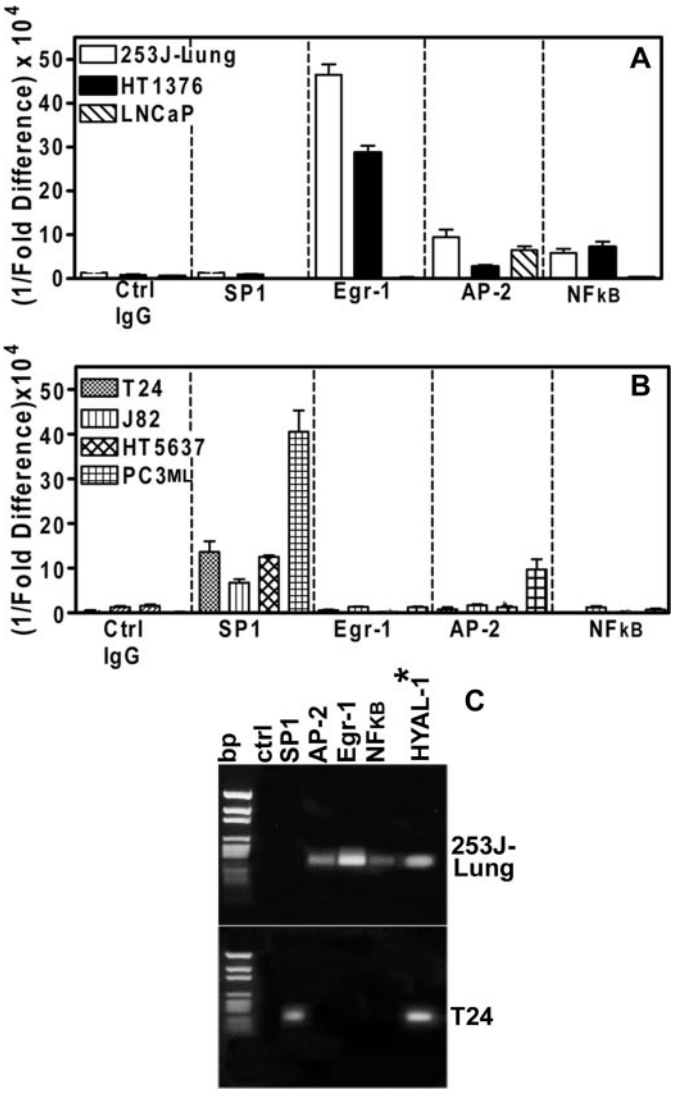

FIGURE 6. **Examination of transcription factor binding to HYAL-1 promoter by CHIP assay.** Formaldehyde-fixed and sonicated lysates of bladder and prostate cancer cells were subjected to CHIP assays using normal rabbit IgG (*Ctrl IgG*), or IgGs for anti-SP1, anti-Egr-1, anti-AP-2, and anti-NFκB. Following CHIP, immunoprecipitated DNA was subjected to real time PCR using HYAL-1 primers (−146L and +84R) that amplify the HYAL-1 promoter region, as described under "Experimental Procedures." *A*, real time PCR assay results; *B*, agarose gel electrophoresis of the real time PCR samples of 253J-Lung and T24 cells shown under "*A*." *C*, *HYAL-1**, PCR product generated by PCR amplification of the −146L/+84R promoter construct, in the same real time PCR experiment.

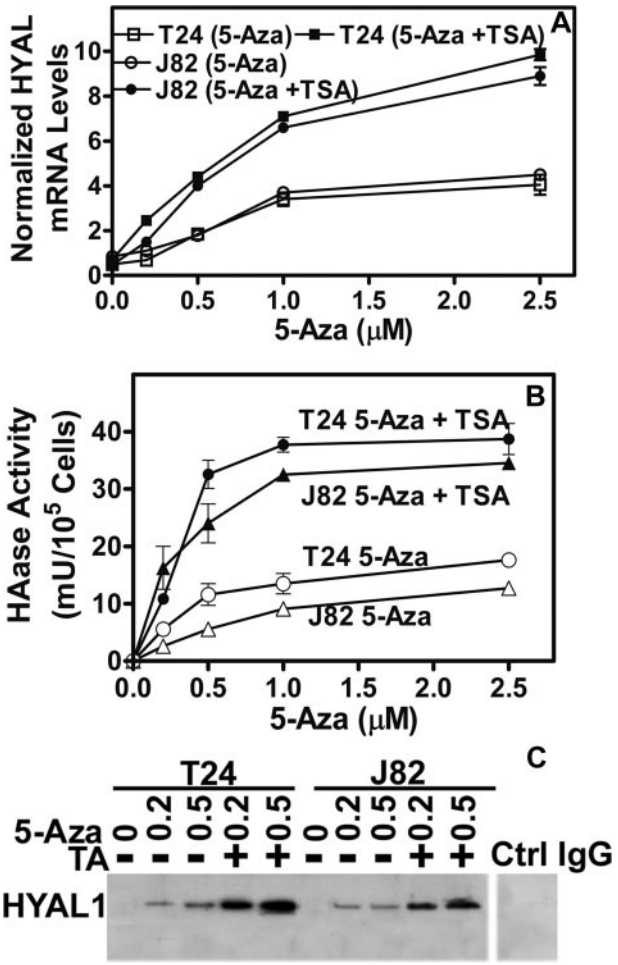

FIGURE 7. **Examination of HYAL-1 expression and HAase activity following 5-AzaC and TSA treatment.** T24 and J82 cells were treated with 5-AzaC either alone or in combination with TSA (100 nM) as described under "Experimental Procedures." *A,* measurement of HYAL-1 mRNA expression by RT-real time PCR; *B,* measurement of HAase activity in the CM of 5-AzaC-treated or untreated T24 and J82 cells by the HAase ELISA-like assay. *C,* immunoblot analysis of HYAL-1 protein in T24 and J82 cell CM following 5-AzaC and TSA treatment.

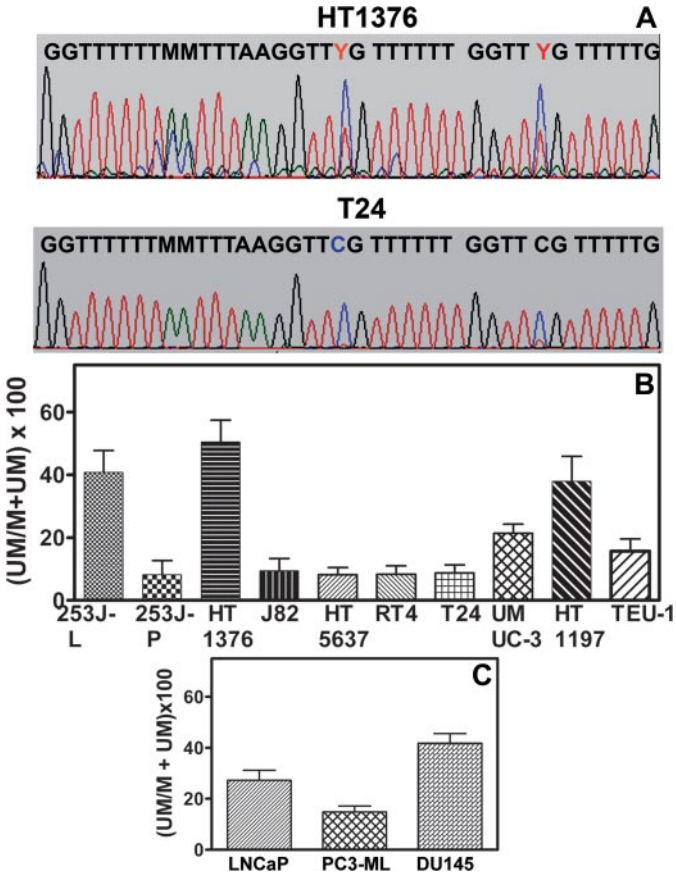

FIGURE 8. **Analysis of HYAL-1 promoter methylation.** Genomic DNA isolated from bladder and prostate cells was treated with sodium bisulfite and subjected to direct sequencing or methylation-specific real time PCR as described under "Experimental Procedures." *A,* sequencing of bisulfite-treated DNA. HYAL-1 promoter region was amplified from bisulfite-treated DNA by PCR and then sequenced using the −224(BS)L primer as described under "Experimental Procedures." *B* and *C,* bisulfite-treated DNA was subjected to real time PCR using the −224(BS)L and +25(BS)R primers and −M(−70) and UM(−70) probes to distinguish between methylated and unmethylated C^{-71} and C^{-59}.

HYAL-1 protein levels. As shown in Fig. 7*B*, 5-AzaC alone increases HAase activity from undetectable levels to up to 5–10 milliunits/10^5 cells, whereas, together with TSA, the HAase levels are similar to those secreted by HYAL-1-expressing 253J-Lung and HT1376 cells (~20–40 milliunits/10^5 cells). As shown in Fig. 5*C*, 5-AzaC induces HYAL-1 protein expression in T24 and J82 cells, and the expression is increased further in the presence of TSA. Similar results were also observed in other low HYAL-1-expressing cells (*i.e.* 253J-parent, HT5637; data not shown). These results show that the endogenous HYAL-1 expression is regulated by DNA methylation. It is noteworthy that because CpG methylation does not occur in prokaryotes, various HYAL-1 reporter constructs tested in this study were unmethylated and therefore showed comparable promoter activity in bladder and prostate cells, regardless of the methylation status of the endogenous HYAL-1 promoter.

Analysis of HYAL-1 Promoter Methylation—To determine whether HYAL-1 promoter methylation occurs at C^{-71}, C^{-59}, and/or C^{-6}, genomic DNA isolated from bladder and prostate cancer cells was treated with sodium bisulfite and then sequenced. As shown in Fig. 8*A*, in HT1376 cells, both C^{-71} and C^{-59} are partially methylated (both C and T peaks are detected). However, in T24 cells, both C^{-71} and C^{-59} are methylated. In both cell lines, C^{-6} was methylated (data not shown). To quantify methylation at C^{-71} and C^{-59} in bladder and prostate cancer cell lines, we performed methylation-specific real time PCR (37, 38) using primers that amplify the bisulfite-modified HYAL-1 promoter region and detection probes that distinguish between methylated and unmethylated C^{-71} and C^{-59}. As shown in Fig. 8*B*, in HYAL-1-expressing bladder cancer cells, the percentage of unmethylated $C^{-71} + C^{-59}$ is 4–7-fold higher than in low to no HYAL-1-expressing cells. Furthermore, the difference between the percentage of unmethylated $C^{-71} + C^{-59}$ in HYAL-1-expressing cells (*i.e.* HT1376, 253J-Lung, HT1197, and UMUC-3) and in HYAL-1 nonexpressing cells (*i.e.* 253J-Parent, RT4, T24, TEU1, and HT5637) is statistically significant ($p < 0.001$; Bonferroni's test). Similarly, in prostate cancer cells, the percentage of unmethylated $C^{-71} + C^{-59}$ in low HYAL-1-expressing PC3-ML is 2–3-fold higher than in HYAL-1 expressing LNCaP and DU145 cells, respectively. Furthermore, Pearson's correlation analysis showed that

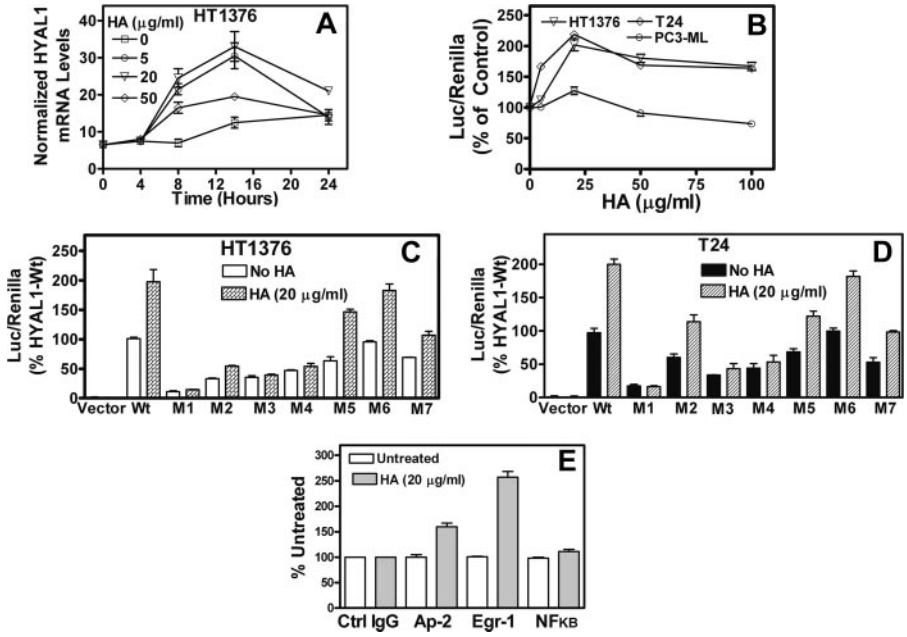

FIGURE 9. **Effect of HA on HYAL-1 expression, HYAL-1-promoter activity, and transcription factor binding.** *A,* effect of HA on HYAL-1 expression. HT1376 cells were treated with various concentrations of HA for different time periods, and HYAL-1 mRNA expression was examined by real time RT-PCR analysis, as described under "Experimental Procedures." HYAL-1 mRNA expression was normalized to β-actin mRNA expression. *B,* bladder and prostate cancer cells co-transfected with the −93/+84 and *Renilla* vector were exposed to various concentrations of HA for 14 h. The normalized firefly luciferase activity in the untreated control is considered as 100%, and the results of the treated samples are expressed as percent of untreated. *C* and *D,* effect of HA on the promoter activity of vector, HYAL-1 wild type, and oligonucleotide mutants. HT1376 (*C*) and T24 (*D*) cells were transiently transfected with vector, HYAL-1 wild type, and an oligonucleotide mutant (described in Fig. 5*A*). 48 h following transfection, the cells were treated with HA (20 μg/ml) for 14 h, and the firefly and *Renilla* luciferase activities were determined as described under "Experimental Procedures." The normalized firefly luciferase activity in the untreated HYAL-1 wild type construct transfected cells is considered as 100%, and the results of all other samples are expressed as percent of HYAL-1 wild type (*HYAL-1-Wt*). *E,* effect of HA on transcription factor binding to HYAL-1 promoter by CHIP assay. HT1376 cells were treated with 20 μg/ml HA for 14 h. Following treatment, the cell lysates were subjected to CHIP assay using normal rabbit IgG (*Ctrl IgG*) or IgGs for anti-Eg-1, anti-AP-2, and anti-NFκB. Following CHIP, immunoprecipitated DNA was subjected to real time PCR using −146L and +84R primers as described under "Experimental Procedures." The results are expressed as percent untreated, where the 1/fold difference × 10^4 for the untreated sample for each IgG was considered as 100%. The mean (1/fold difference) × 10^4 for the untreated samples are as follows: 0.837 (rabbit IgG), 2.72 (AP-2), 28.72 (Egr-1), and 7.18 (NFκB).

in bladder and prostate cells, the correlation between the percentage of unmethylated C^{-71} + C^{-59} and HAase activity (as shown in Fig. 1) is statistically significant (Spearman $r = 0.879$; $p < 0.0001$; two-tailed). We also attempted to use detection probes that distinguish methylated and unmethylated C^{-71} and C^{-59} separately. However, these probes could not distinguish the methylation status at single nucleotides even in the bisulfite-treated HYAL-1 promoter standard (−146/+84 construct) that was unmethylated or methylated *in vitro* using the M.SssI DNA methylase (data not shown).

Effect of HA and HA-oligo on HYAL-1 Promoter Activity—Because very little is known about the regulation of HYAL-1 expression, we examined whether HYAL-1 expression is under the regulation of its own substrate (*i.e.* HA) or the degradation product (*i.e.* HA-oligo ~2 kDa). We examined their effect on HYAL-1 mRNA expression by real time RT-PCR. As shown in Fig. 9*A*, HA increases HYAL-1 expression in HT1376 cells in a dose-dependent manner, with a maximum increase of ~3-fold observed at 20 μg/ml concentration, at the 14-h time point. HA-oligo did not alter HYAL-1 mRNA expression when tested at similar concentrations and time intervals (data not shown). HA also did not cause any induction in HYAL-1 mRNA expression in T24 or J82 cells, which show little HYAL-1 expression. We next examined the effect of HA on HYAL-1 promoter activity in HT1376, T24, and PC3-ML cells transfected with the −93/+84 construct. Because HA caused a maximum increase in HYAL-1 mRNA levels at 20 μg/ml concentration after 14 h of incubation, we used these conditions to examine the effect of HA on HYAL-1 promoter activity. As shown in Fig. 9*B*, HA increases HYAL-1 promoter activity in both T24 and HT1376 cells in a dose-dependent manner with a maximum increase of ~2.3-fold ($p < 0.01$; Bonferroni's multiple comparison test). In PC3-ML cells that express high HA levels (20), HA did not increase HYAL-1 promoter activity and, at higher concentration, a slight decrease (~25%) was observed (Fig. 9*B*). The increase in HYAL-1 promoter activity by HA was observed with two different sources of HA (*i.e.* human umbilical cord HA and HA prepared by bacterial fermentation (Genzyme Corp.)). As in the case of HYAL-1 mRNA expression, the HA-oligo did not induce any HYAL-1 promoter activity.

To determine which sequence in the minimal HYAL-1 promoter region is responsible for HA-induced increase in HYAL-1 expression, we examined the effect of HA on HYAL-1 promoter activity induced by HYAL-1 wild type promoter and promoter mutant constructs. As shown in Fig. 9*C*, in HT1376 cells, HA causes ~2-fold induction of the promoter activity displayed by the wild type construct. However, HA does not cause any increase in the promoter activity of mutants M1, M3, and M4. In contrast, HA increases the promoter activity of mutants M2, M5, M6, and M7. As described in Fig. 5, M1 lacks the $CC^{-71}GCC$ site; in M3, both C^{-71} and C^{-59} are mutated, and in M4, C^{-71} is mutated. This suggests that HA most likely induces HYAL-1 promoter activity through the Egr-1-binding site that involves C^{-71}. Similar results are also obtained in T24 cells, suggesting that in both HYAL-1-expressing and nonexpressing cells (Fig. 9*D*), HA induces promoter activity through the same mechanism. We next used the CHIP assay to examine whether HA increased the binding of certain transcription factors to the HYAL-1 promoter in HT1376 cells. As shown in Fig. 9*E*, HA increased the binding of Egr-1 (~2.5-fold) and to a lesser extent of AP-2 (1.6-fold) to the HYAL-1 promoter, and this increase was statistically significant ($p < 0.01$; *t* test). HA treatment induced very little increase (1.2-fold) in NFκB binding to the HYAL-1 promoter in HT1376 cells (Fig.

9*E*). Consistent with the finding that HA did not induce HYAL-1 expression in HYAL-1 nonexpressing cells, HA did not alter SP1 binding to the HYAL-1 promoter in T24 cells. Furthermore, HA did not induce Egr-1, AP-2, or NFκB binding to the HYAL-1 promoter in T24 cells (data not shown). These results show that although HA increases HYAL-1 expression in cells that normally express HYAL-1, it does not induce HYAL-1 expression in HYAL-1 nonexpressing cells. This suggests that the binding of different transcription factors to the methylated and unmethylated HYAL-1 promoter is the key regulator of HYAL-1 expression in bladder and prostate cancer cells.

DISCUSSION

HYAL-1 HAase is overexpressed in a variety of carcinomas such as bladder, prostate, head and neck, and breast. Furthermore, elevated HYAL-1/HAase levels are an accurate diagnostic and prognostic marker for cancer progression (12–23, 39). HYAL-1 is involved in promoting tumor growth, infiltration, and angiogenesis (24, 25, 40). However, the overexpression of HYAL-1, at concentrations much higher than those usually expressed in tumor tissues and tumor cells, induces apoptosis and inhibits tumor formation (25). Besides these studies, there is little information about how HYAL-1 expression is regulated.

Our study shows that in normal and tumor tissues and cells, HYAL-1 expression is controlled mainly at the transcription level. HYAL-1 mRNA levels in high HYAL-1-expressing cells are 10–50-fold greater than in low HYAL-1-expressing cells. Furthermore, HYAL-1 mRNA levels in bladder tumor tissues are 6–10-fold higher than in normal bladder tissues. We have previously shown that in tumor tissues, HYAL-1 is exclusively expressed in tumor cells (13, 16, 19, 20). Therefore, the elevated HYAL-1 levels in tumor tissues are most likely attributed to the increased HYAL-1 expression in tumor cells. It is noteworthy that HYAL-1 expression is low in normal bladder specimens (as compared with bladder tumor specimens) from patients with active bladder cancer. This suggests that HYAL-1 is most likely not turned on as a result of the "field effect." Field effect has been suggested to prime the entire urothelium for developing tumors because of the prolonged exposure of the urothelium to carcinogens, such as those in cigarette smoke or paints and dyes (41).

Analysis of TSS shows that HYAL-1 is expressed in a variety of normal tissues and that there are multiple TSS. In the majority of tissues, including bladder and prostate tissues/cells, transcription starts between nucleotides −1 and +5. These TSS are 30–36 bases downstream of the canonical TACAAA box. TACAAA is a weak TATA box with the TATA-binding proteins interacting at the TACA sequence (42, 43). No canonical TACAAA or TATA box is found upstream of any of the other TSS (*i.e.* −450, −30, +41, +65, +377, and +550). It is noteworthy that HYAL-2 transcription also starts at multiple TSS but no canonical TATA box is found within the HYAL-2 gene (26). At the present time, the function of the untranslated nucleotide sequence between +1 and +616 is unknown. However, the detection of TSS at +41, +65, +377, and +550 nucleotides indicates that at least in some tissues, this untranslated leader sequence is necessary for HYAL-1 transcription.

The region between nucleotides −93 and +84 (the −93/+84 construct) is equally effective at inducing the reporter activity in bladder and prostate cancer cell lines that either express high HYAL-1 levels (*e.g.* 253J-Lung, HT1376, and DU145), moderate HYAL-1 levels (*e.g.* UMUC-3, 253J-Parent, and LNCaP), or very low/no HYAL-1 (*e.g.* T24, J82, HT5637, and PC3-ML). This discrepancy between endogenous HYAL-1 expression and HYAL-1-reporter activity can be explained by the fact that methylation of the HYAL-1 promoter at C^{-71} and C^{-59} inversely correlates with the endogenous HYAL-1 expression. Because in prokaryotes there is no CpG methylation, the HYAL-1-promoter constructs are unmethylated and therefore induce HYAL-1 promoter activity regardless of the methylation status of the endogenous HYAL-1 promoter.

DNA hypermethylation is often associated with silencing of tumor suppressor genes, and it involves a CpG island (35). In contrast, HYAL-1 promotes tumor growth, invasion, and angiogenesis, and the promoter contains no CpG island (24, 25). Similar to HYAL-1, heparanase, which degrades heparan sulfate, promotes tumor growth and progression (44, 45). DNA methylation is the main epigenetic event for heparanase regulation in cancer (46, 47). In bladder and prostate carcinomas, heparanase expression inversely correlates with the methylation of an Egr-1-binding site (46, 48). DNA hypomethylation occurs commonly in cancer, especially in bladder cancer, and it induces the expression of genes involved in tumor growth and progression (49–52). It is noteworthy that such hypomethylation occurs at CpGs within a promoter, but these CpGs are not part of a CpG island (49). Thus, DNA hypomethylation may induce the expression of glycosaminoglycan-degrading enzymes such as HYAL-1 and heparanase that promote tumor invasion and angiogenesis (40, 44, 53).

Because HYAL-1 promoter activity was low in normal urothelial cells, it suggests that the nuclear environment (*e.g.* transcription factor expression/activation) is important in regulating HYAL-1 expression. CHIP assay results show that in cells that express HYAL-1, Egr-1 (and to a lesser degree AP-2) binds to the HYAL-1 promoter. Egr-1 and AP-2 consensus sites are present between nucleotides −73 and −50. Because the deletion of the $CC^{-71}GCCC$ site leads to ~90% reduction in HYAL-1 promoter activity, the binding of Egr-1 (and possibly Ap-2) to this site appears to be necessary for the induction of HYAL-1 promoter activity. On the contrary, in cells which do not express HYAL-1, we found SP1 binding to the HYAL-1 promoter. Because both SP1 and Egr-1 have two overlapping binding sites within the promoter (Fig. 5), it appears that although SP1 binding to the methylated HYAL-1 promoter turns off transcription, binding of Erg-1 (and also AP-2) to the unmethylated promoter turns on transcription. Furthermore, binding of NFκB to its consensus sequence is not necessary for turning on transcription, but it may enhance the promoter activity. The lack of Egr-1 binding to the HYAL-1 promoter in LNCaP cells may be due to the lower percentage of unmethylated C^{-71} and C^{-59} in the HYAL-1 promoter (Fig. 8). This also may explain why HYAL-1 expression is lower in LNCaP cells when compared with the expression in 253J-Lung, HT1376, or DU145 cells.

Identification of the minimal promoter region in the HYAL-1 gene should allow the evaluation of the regulation of

HYAL-1 expression in normal and tumor tissues. We found that HA induces HYAL-1 expression and also the promoter activity. The mechanism of HA-induced HYAL-1 expression most likely involves increased binding of transcription factors Egr-1, AP-2, and to a lesser extent of NFκB to the HYAL-1 promoter. In contrast, the ~2-kDa HA-oligo, which is the end product of HA degradation by HYAL-1, does not have any effect on HYAL-1 expression or promoter activity. The modest induction (2–2.5-fold) of HYAL-1 expression and promoter activity by HA may be because the bladder and prostate cancer cells used in this study also synthesize and secrete HA (20, 32). Thus, the exogenous addition of HA may only have a moderate effect on the overall induction of HYAL-1 by HA.

Taken together, in this study we established that the elevated expression of HYAL-1 protein and HAase levels in tumor cells and high grade tumor tissues is mainly because of increased HYAL-1 mRNA levels. The minimal HYAL-1 promoter region contains overlapping transcription factor binding sites, and these sequences are important for the promoter activity. HYAL-1 expression appears to be epigenetically regulated. Promoter methylation and the binding of different transcription factors to the methylated and unmethylated promoter appear to be the key regulators of HYAL-1 expression in normal and tumor cells. Our study also raises an interesting question about cancer therapeutics involving DNA-demethylating agents. Hyper-methylation of tumor suppressor genes has been extensively investigated for developing cancer markers and therapeutics. However, if DNA hypo-methylation turns on the genes that function in tumor growth and metastasis (*e.g.* heparanase, urokinase-type plasminogen activator, MMP-2, HYAL-1), then DNA hypo-methylation-inducing therapies may only have short term efficacy, as they could speed up the progression of surviving cancer cells (49). Identification of the HYAL-1 promoter and plausible mechanisms of promoter regulation should allow future studies on how various environmental and cellular factors and DNA-demethylating treatments affect HYAL-1 expression in normal and disease conditions.

Acknowledgments—We thank Joe Ferreira, David Grant, and Dr. Susan Ganz and their organ retrieval team at the University of Miami. We thank Dr. Todd Miller, Sr. Research Scientist, Specialty Laboratories, Valencia, CA, for advice on promoter cloning strategy. We are grateful to Dr. Kavitha Ramachandran and Dr. Rakesh Singal, University of Miami Miller School of Medicine, and Michael Wu, Millipore Corp., for their advice regarding CHIP assay. We gratefully acknowledge the editorial assistance of Cynthia Soloway.

REFERENCES

1. Stern, R., Asari, A. A., and Sugahara, K. N. (2006) *Eur. J. Cell Biol.* **85,** 699–715
2. Stern, R., and Jedrzejas, M. J. (2006) *Chem. Rev.* **106,** 818–839
3. Toole, B. P. (2004) *Nat. Rev. Cancer* **4,** 528–539
4. Toole, B. P., Zoltan-Jones, A., Misra, S., and Ghatak, S. (2005) *Cells Tissue Organs* **179,** 66–72
5. Hascall, V. C., Majors, A. K., De La Motte, C. A., Evanko, S. P., Wang, A., Drazba, J. A., Strong, S. A., and Wight, T. N. (2004) *Biochim. Biophys. Acta* **1673,** 3–12
6. Tammi, M. I., Day, A. J., and Turley, E. A. (2002) *J. Biol. Chem.* **277,** 4581–4584
7. Slevin, M., Krupinski, J., Gaffney, J., Matou, S., West, D., Delisser, H., Savani, R. C., and Kumar, S. (2007) *Matrix Biol.* **26,** 58–68
8. Stern, R. (2005) *Pathol. Biol.* **53,** 372–382
9. Csoka, A. B., Frost, G. I., and Stern, R. (2001) *Matrix Biol.* **20,** 499–508
10. Csóka, A. B., Frost, G. I., Wong, T., and Stern, R. (1997) *FEBS Lett.* **417,** 307–310
11. Frost, G. I., Csóka, A. B., Wong, T., and Stern, R. (1997) *Biochem. Biophys. Res. Commun.* **236,** 10–15
12. Schroeder, G. L., Lorenzo-Gomez, M. F., Hautmann, S. H., Friedrich, M. G., Ekici, S., Huland, H., and Lokeshwar, V. (2004) *J. Urol.* **172,** 1123–1126
13. Hautmann, S. H., Lokeshwar, V. B., Schroeder, G. L., Civantos, F., Duncan, R. C., Gnann, R., Friedrich, M. G., and Soloway, M. S. (2001) *J. Urol.* **165,** 2068–2074
14. Aboughalia, A. H. (2006) *Arch. Med. Res.* **37,** 109–116
15. Eissa, S., Kassim, S. K., Labib, R. A., El-Khouly, I. M., Ghaffer, T. M., Sadek, M., Razek, O. A., and El-Ahmady, O. (2005) *Cancer* **103,** 1356–1362
16. Posey, J. T., Soloway, M. S., Ekici, S., Sofer, M., Civantos, F., Duncan, R. C., and Lokeshwar, V. B. (2003) *Cancer Res.* **63,** 2638–2644
17. Ekici, S., Cerwinka, W. H., Duncan, R., Gomez, P., Civantos, F., Soloway, M. S., and Lokeshwar, V. B. (2004) *Int. J. Cancer* **112,** 121–129
18. Franzmann, E. J., Schroeder, G. L., Goodwin, W. J., Weed, D. T., Fisher, P., and Lokeshwar, V. B. (2003) *Int. J. Cancer* **106,** 438–445
19. Lokeshwar, V. B., Young, M. J., Goudarzi, G., Iida, N., Yudin, A. I., Cherr, G. N., and Selzer, M. G. (1999) *Cancer Res.* **59,** 4464–4470
20. Lokeshwar, V. B., Rubinowicz, D., Schroeder, G. L., Forgacs, E., Minna, J. D., Block, N. L., Nadji, M., and Lokeshwar, B. L. (2001) *J. Biol. Chem.* **276,** 11922–11932
21. Lokeshwar, V. B., Obek, C., Pham, H. T., Wei, D., Young, M. J., Duncan, R. C., Soloway, M. S., and Block, N. L. (2000) *J. Urol.* **163,** 348–356
22. Pham, H. T., Block, N. L., and Lokeshwar, V. B. (1997) *Cancer Res.* **57,** 778–783; Correction (1997) *Cancer Res.* **57,** 1622
23. Lokeshwar, V. B., Schroeder, G. L., Selzer, M. G., Hautmann, S. H., Posey, J. T., Duncan, R. C., Watson, R., Rose, L., Markowitz, S., and Soloway, M. S. (2002) *Cancer* **95,** 61–72
24. Lokeshwar, V. B., Cerwinka, W. H., and Lokeshwar, B. L. (2005) *Cancer Res.* **65,** 2243–2250
25. Lokeshwar, V. B., Cerwinka, W. H., Isoyama, T., and Lokeshwar, B. L. (2005) *Cancer Res.* **65,** 7782–7789
26. Chow, G., and Knudson, W. (2005) *J. Biol. Chem.* **280,** 26904–26912
27. Lokeshwar, V. B., Schroeder, G. L., Carey, R. I., Soloway, M. S., and Iida, N. (2002) *J. Biol. Chem.* **277,** 33654–33663
28. Lokeshwar, V. B., Estrella, V., Lopez, L., Kramer, M., Gomez, P., Soloway, M., and Lokeshwar, B. (2006) *Cancer Res.* **66,** 11219–11227
29. Selbi, W., de la Motte, C., Hascall, V., and Phillips, A. (2004) *J. Am. Soc. Nephrol.* **15,** 1199–1211
30. Ohno, S., Ijuin, C., Doi, T., Yoneno, K., and Tanne, K. (2002) *J. Periodontol.* **73,** 1331–1337
31. Li, L., Asteriou, T., Bernert, B., Heldin, C. H., and Heldin, P. (2007) *Biochem. J.* **404,** 327–336
32. Golshani, R., Hautmann, S. H., Estrella, V., Cohen, B. L., Kyle, C. C., Manoharan, M., Jorda, M., Soloway, M. S., and Lokeshwar, V. B. (2007) *Int. J. Cancer* **120,** 1712–1720
33. Das, P. M., Ramachandran, K., Vanwert, J., Ferdinand, L., Gopisetty, G., Reis, I. M., and Singal, R. (2006) *Mol. Cancer* **5,** 28
34. Xue, Y., Zhou, F., Fu, C., Xu, Y., and Yao, X. (2006) *Nucleic Acids Res.* **34,** W254–W257
35. Frost, G. I., Mohapatra, G., Wong, T. M., Csóka, A. B., Gray, J. W., and Stern, R. (2000) *Oncogene* **9,** 870–877
36. Das, P. M., and Singal, R. J. (2004) *Clin. Oncol.* **22,** 4632–4642
37. Sasaki, M., Anast, J., Bassett, W., Kawakami, T., Sakuragi, N., and Dahiya, R. (2003) *Biochem. Biophys. Res. Commun.* **309,** 305–309
38. Li, L. C., and Dahiya, R. (2002) *Bioinformatics* (*Oxf.*) **18,** 1427–1431
39. Poola, I., Abraham, J., Marshalleck, J. J., Yue, Q., Lokeshwar, V., Bonney, G., and DeWitty, R. L. (2008) *Clin. Cancer Res.* **14,** 1274–1280
40. Simpson, M. A. (2006) *Am. J. Pathol.* **169,** 247–257
41. Droller, M. J. (2002) *Urol. Clin. North Am.* **29,** 229–234
42. Meyer, T., Carlstedt-Duke, J., and Starr, D. B. (1997) *J. Biol. Chem.* **272,**

30709–30714
43. Klug, J., and Beato, M. (1996) *Mol. Cell. Biol.* **16,** 6398–6407
44. Vlodavsky, I., Abboud-Jarrous, G., Elkin, M., Naggi, A., Casu, B., Sasisekharan, R., and Ilan, N. (2006) *Pathophysiol. Haemost. Thromb.* **35,** 116–127
45. Naomoto, Y., Takaoka, M., Okawa, T., Nobuhisa, T., Gunduz, M., and Tanaka, N. (2005) *Oncol. Rep.* **14,** 3–8
46. Ogishima, T., Shiina, H., Breault, J. E., Terashima, M., Honda, S., Enokida, H., Urakam, S., Tokizane, T., Kawakami, T., Ribeiro-Filho, L. A., Fujime, M., Kane, C. J., Carroll, P. R., Igawa, M., and Dahiya, R. (2005) *Oncogene* **24,** 6765–6772
47. Shteper, P. J., Zcharia, E., Ashhab, Y., Peretz, T., Vlodavsky, I., and Ben-Yehuda, D. (2003) *Oncogene* **22,** 7737–7749
48. Ogishima, T., Shiina, H., Breault, J. E., Tabatabai, L., Bassett, W. W., Enokida, H., Li, L. C., Kawakami, T., Urakami, S., Ribeiro-Filho, L. A., Terashima, M., Fujime, M., Igawa, M., and Dahiya, R. (2005) *Clin. Cancer Res.* **11,** 1028–1036
49. Ehrlich, M. (2002) *Oncogene* **21,** 5400–5413
50. Seifert, H. H., Schmiemann, V., Mueller, M., Kazimirek, M., Onofre, F., Neuhausen, A., Florl, A. R., Ackermann, R., Boecking, A., Schulz, W. A., and Grote, H. J. (2006) *Exp. Mol. Pathol.* **82,** 292–297
51. Shukeir, N., Pakneshan, P., Chen, G., Szyf, M., and Rabbani, S. A. (2006) *Cancer Res.* **66,** 9202–9210
52. Schulz, W. A., and Hatina, J. (2006) *J. Cell. Mol. Med.* **10,** 100–125
53. Simpson, M. A., and Lokeshwar, V. B. (2008) *Front. Biosci.* **13,** 5664–5680